SAND2015-4809C

Space-filtered kinetic theory for the LES of dense sprays

F. Doisneau[1,⋆], M. Arienti[1], J. C. Oefelein[1]
[1]Combustion Research Facility, Sandia National Laboratories, Livermore CA 94551-0969, USA
⋆Corresponding Author Email: fdoisne@sandia.gov

Abstract

Kinetic theory is often used as a framework to derive moment equations for sprays, with considerable success in the case of a dilute spray in a fully resolved (DNS) gas field. In the prospect of computing LES of atomization with a spray solver, a formalism that accounts for the non-linear interaction between high-loading regions and turbulence at the subfilter level is needed. So we first introduce an extended kinetic theory frame, where the phase space is extended to space-filtered spray quantities. This rigorous formalism is a comprehensive baseline but it requires additional closures. Second we quantify through *a priori DNS* the behavior of segregation as a relevant space-filtered quantity to describe the spray's subfilter behavior. Third we discuss an assumption on the subfilter spray structures which allows the closure of drag, heating, and collisions from the sole knowledge of segregation.

Keywords: Dense spray, cluster segregation, Large Eddy Simulation, Williams-Boltzmann equation

---

1 Introduction

Dense sprays can be found in various mechanical engineering systems such as near the atomization region of a liquid fuel injector. It is well known that dilute sprays (one-way coupled) encounter preferential concentration [2] which phenomenon has been widely studied and little modeled. In dense regions however, the loading of the disperse phase is high enough to drive, together with the carrier phase, the overall flow: both large scales and small scales exhibit specific hydrodynamic and thermal dynamics, which we refer to as two-way coupling. Understanding all the scales of such flows is key to designing Gasoline, Diesel, and RCCI combustion chambers and especially injectors. Especially Large Eddy Simulation (LES) of the injection in the Engine Combustion Network's Spray A case [18] is a short term goal and requires the modeling of the two-phase small scales.

The granular flow [1] and fluidized bed [3, 17] communities have given, in denser cases, some insight on preferential concentration, sometimes referred to as clustering. At the small scale level, droplets are known -from dilute studies- to follow trajectories which complexity increases with their inertia but they now drag the flow depending on their local loading, alternatively triggering more small scales and disrupting them in the carrier phase [9]: we refer to this general behavior as two-phase turbulence. The problem is fully coupled and the modeling and analysis paradigms of traditional turbulence are not applicable: dense two-phase turbulence is a modeling frontier. Of primary interest are the unevenness and fluctuations of the local droplet loading: i) the two-way coupling times and equilibrium values depends on the local loading; ii) the larger droplet concentrations trigger collisions/coalescence/agglomeration. And this unevenness, referred to as segregation, is supported by instability mechanisms: for instance inertial droplets tend to both kill vorticity and accumulate in low vorticity regions, a mechanism acknowledged in the granular flow community and leading to the formation of clusters [1].

The complete and fundamental understanding of these mechanisms is certainly needed but, in the prospect of full-system-simulations of fuel injectors, we seek for a reduced approach that can capture the main features of dense sprays: 1) the essential aspects of the small scale flow to predict turbulent transport and droplet size evolution and 2) the large scale flow as influenced by the small scales. For that, we introduce a space-filtered statistical frame for two-way coupled disperse phase flows focused on the level of clustering as a driving parameter. To foster the relevance of this choice, we lead a first study on the small scale behavior of clustering and we provide large scale closures which rely on a unique subfilter segregation parameter. The main originality of the approach is to rely on the transport of segregation, a low order measure of clustering itself, instead of solving for any turbulent velocity moments as inspired from single-phase RANS and LES. We give the argument that the two-phase scales can be described with a single cluster characteristic time and size instead of resorting to an multi-scale spectrum at equilibrium: a complete first model is made consistent to this unique (subfilter) scale.

The paper is organized as follows: in Section 2 a space-filtered statistical formalism is derived for the two-way coupled fluid-kinetic description of dense sprays, with the extension of the phase space to filtered

segregation, leading to the Extended Filtered Fluid-Kinetic formalism; in Section 3, an *a priori* DNS study of a model two-way coupled free turbulence leads to a closure for the evolution of the filtered segregation; in Section 4, we introduce an assumption allowing to derive closures for the filtered source terms of the fluid-kinetic equations, we propose a model for drag and heating, and we discuss the merits and limitations of the segregation-based closure for collisions and vaporization. We finally conclude and discuss the further modeling efforts to be conducted to provide an LES tool for dense sprays.

2 A new approach for the LES of moderately dense sprays

From the classical statistical formalism for a flow of many liquid particles (noted with index l) suspended in a carrier phase (a gas, noted with index g), we introduce a space-filtered formalism and justify its relevance to the LES of sprays.

2.1 Fluid-kinetic formalism

The whole information about a disperse phase can be cast into a number density function (NDF), normalized to N_p the number of particles. The aspects of treating non-spherical drops (blobs) are left aside so that the dense spray is re-qualified as a moderately dense spray [6]: the volume fraction should remain below one in most of the domain. The NDF is noted $f(t, \boldsymbol{x}; \boldsymbol{c}, \theta, r)$ with $f\mathrm{d}\boldsymbol{c}\mathrm{d}\theta\mathrm{d}r$ the number of particles in a volume between $\boldsymbol{x}$ and $\boldsymbol{x}+\mathrm{d}\boldsymbol{x}$ with a velocity between $\boldsymbol{c}$ and $\boldsymbol{c}+\mathrm{d}\boldsymbol{c}$, a temperature between θ and $\theta+\mathrm{d}\theta$, and a radius between r and $r+\mathrm{d}r$. This NDF is a smooth, Eulerian field, thanks to the fact it is average over an infinite ensemble of realizations of the particulate flow. The question of the relevance of this approach in two-way coupled contexts is not solved yet [21] and it is not discussed here. The NDF follows the celebrated Williams-Boltzmann equation:

$$\partial_t f + \partial_{\boldsymbol{x}} \cdot (\boldsymbol{c} f) + \partial_{\boldsymbol{c}} \cdot (\mathbf{F} f) + \partial_\theta \left(\frac{\mathrm{H}}{c_{p,l}} f \right) + \partial_r (R_r f) = \mathfrak{B}(f) + \mathfrak{C}(f, f) \tag{1}$$

which is a class of kinetic equation. This equation is coupled to the carrier phase through the exchange terms $\mathbf{F}$ (drag), H (heating), and R_r (vaporization) and through $\mathfrak{B}$ (break-up) and $\mathfrak{C}$ (coalescence) if the latter are closed with dependencies on the local gas conditions (aerodynamic Weber number, collision efficiencies). As a counterpart, the carrier phase encounters significant transfer of mass heat and momentum above a certain local mass loading of the spray, which are accounted for through source terms in the carrier phase equations. In this case, the problem is said to be two-way coupled and it requires more care on both modeling and resolution sides. This peculiar system is referred to as fluid-kinetic. We pick the Navier-Stokes equations to describe the carrier phase so our fluid-kinetic formalism to describe two-way coupled sprays is the system composed of the coupled Navier-Stokes system and Williams-Boltzmann equation.

The requirements for a fluid-kinetic DNS which aims at fully resolving the carrier phase and NDF fields (and therefore the gradients) are then $\Delta x < \min(\eta, \eta_p)$ where η is the Kolmogorov length scale of the carrier phase realization. The length scale η_p of spatial variation of f can be arbitrarily small (even below r) but it is unlikely lower than η since the particle field is driven by the gas.

2.2 The filtered fluid-kinetic (FFK) formalism

Several attempts have been made to filter two-phase models [16]. We here introduce a general and rigorous approach, which relies on kinetic theory. The spirit of LES is not only to remove small structures but also to get rid of part of the variability (realization variance) of the flows. Recognizing the previous facts, it is desirable to filter some details away from the fluid-kinetic system. We define an LES filtering in the classical way [19] from a filter function $g_{\Delta x}(\boldsymbol{x})$ with a cut-off length Δx:

$$\langle \cdot \rangle_x = \int_{\boldsymbol{x} \in \Omega_x} \cdot \, g_{\Delta x}(\boldsymbol{x} - \boldsymbol{x}') \mathrm{d}\boldsymbol{x}' \quad \text{with} \quad \langle 1 \rangle_x = 1 \tag{2}$$

where $\langle \cdot \rangle_x$ still depends on the physical space variable $(t, \boldsymbol{x})$ as usual but also on the phase spaces ones $(\boldsymbol{c}, \theta, r)$ whenever $\cdot$ does. For some useful variables, we also take the alternative notation $\overline{\cdot} \equiv \langle \cdot \rangle_x$. We then define the Favre and the NDF-weighted space-filters $\widetilde{\cdot} = \frac{\langle \cdot \rho_g(t,x) \rangle_x}{\langle \rho_g(t,x) \rangle_x}$ and $\widehat{\cdot} = \frac{\langle \cdot f \rangle_x}{\langle f \rangle_x}$, the latter being defined in the Favre spirit though it will have additional dependency on the phase space variables: the NDF-weighted filtered quantities are conditioned by particle velocities $\boldsymbol{c}$, temperatures θ, sizes r *etc*. The crucial need to make a distinction between these two "phase operators" has been extensively discussed for RANS models in [11], for Reynolds averaging instead of space filtering. As the same matter of fact, we expect that $\overline{\cdot} \neq \widetilde{\cdot} \neq \widehat{\cdot}$.

The fluid-kinetic equations must be space-filtered simultaneously to preserve the hope of accounting properly for the strong couplings. The phase space variables commute with the physical space filter so that the structure of the phase space (its high-dimension and variables) is preserved by space filtering i.e. we have $\widehat{\boldsymbol{c}} = \boldsymbol{c}$, $\widehat{\theta} = \theta$, and $\widehat{r} = r$. So our particulate phase is now described by the filtered NDF $\overline{f}\,(t, \boldsymbol{x}; \boldsymbol{c}, \theta, r) = \langle f\,(t, \boldsymbol{x}; \boldsymbol{c}, \theta, r)\rangle_x$ which lives on the same phase space as f but has presumably a different shape: especially it is smoother in $\boldsymbol{x}$. The DNS kinetic equation, Eq. (1), was linear in f (apart for the collision/coalescence term) so the filtered kinetic equation formally reads:

$$\partial_t \overline{f} + \partial_{\boldsymbol{x}} \cdot (\boldsymbol{c}\overline{f}) + \partial_{\boldsymbol{c}} \cdot (\widehat{\mathbf{F}}\overline{f}) + \partial_\theta \left(\widehat{\frac{H}{c_{p,l}}} \overline{f} \right) + \partial_r (\widehat{R_r}\overline{f}) = \overline{\mathfrak{B}(f)} + \overline{\mathfrak{C}(f,f)} \tag{3}$$

where the fluxes $\widehat{\mathbf{F}}$, $\widehat{H/c_{p,l}}$, $\widehat{R_r}$ and the sources $\widehat{\mathfrak{B}(f)}$, $\overline{\mathfrak{C}(f,f)}$ are unclosed. Moreover these terms depend on all the physics at the subfilter level. The usual dilute DNS closures resulted directly from far-field integration of single drop solutions but here the multiple scales and their interactions make the dense spray LES closures presumably very different.

2.3 Extending the filtered NDF: the EFFK formalism

To close the unknown terms of Eq. (3), algebraic models can be envisioned [13] as it is done in single phase LES and in some RANS models. solely resorting to the available "resolved" quantities, namely the gas fields $\overline{\rho_g}$, $\widetilde{\boldsymbol{u}_g}$, $\widetilde{T_g}$, $\widetilde{Y_i}$ and the particle filtered information from $\overline{f}$. But the single-phase closures rely on structural properties of turbulence (cascade, scale-similarity, equilibrium spectrum, isotropy) which are presumably not featured by the disperse phase So new closures may be required and/or additional quantities transported. We choose the second option and refer to the resulting formalism as Extended Filtered Fluid-Kinetic (EFFK).

A good example of phase space extension from the literature is the recourse to the gas velocity "seen" by the particles. [8] have described a monodisperse isothermal suspension in turbulence with a kinetic model $f(t, \boldsymbol{x}; \boldsymbol{c}, \boldsymbol{u}_{g@p})$ where $\boldsymbol{u}_{g@p}$ is the carrier phase velocity "seen" or "felt" by the particles [10, 8] and defined as $\boldsymbol{u}_{g@p} = \widehat{\boldsymbol{u}_g}\,(t, \boldsymbol{x})$. Other authors have focused on the budget of some filtered kinetic energies: granular flow theory relies on a granular energy analogous to the microscopic energy in gases [1]: [10] introduces the "Random Uncorrelated Energy" as a unique subfilter energy; and [11] emphasizes the need to separate coherent turbulent energy from the microscopic one.

In the present contribution, we consider the merits of choosing segregation as a transported subfilter quantity: the filtered quantities will evolve in a different manner depending on if the cloud is uniform or clustered in the subfilter due to the many phenomena that are dependent on the local mass or volume fractions. Indeed it is well-known that collisions always depend on the square of the local number concentration but moreover in two-way coupling contexts drag, heat transfer, and evaporation become sensitive to the loading. The subfilter unevenness can be loosely described with the segregation field:

$$\widehat{\text{ш}}(t, \boldsymbol{x}; \boldsymbol{c}, \theta, r) = \frac{\langle\, (f\mathcal{V}(r))^2 \,\rangle_x}{\langle\, f\mathcal{V}(r) \,\rangle_x^2} \tag{4}$$

which is still conditioned by the phase space variables $(\boldsymbol{c}, \theta, r)$. Segregation gives some insight on the space repartition of the droplet cloud at the subfilter level since it depends on the (unknown) DNS NDF f. Of course $\widehat{\text{ш}}$ is dependent on the filter size Δx and should tend to zero with Δx. It must be either estimated (if some structural properties of the flow are known) but we strongly suggest -considering its quantitative impact on closures and in the absence of the fine knowledge of its dynamics- to transport it. In this case, a new model for the creation and destruction of segregation must be sought. The field $\widehat{\text{ш}}$ can be used to define an independent phase space variable simply noted ш which leads to defining the extended filtered NDF:

$$\overline{f}^{\,e}\,(t, \boldsymbol{x}; \boldsymbol{c}, \theta, r, \text{ш}) \quad \text{with of course} \quad \overline{f}\,(t, \boldsymbol{x}; \boldsymbol{c}, \theta, r) = \int \overline{f}^{\,e}\,(t, \boldsymbol{x}; \boldsymbol{c}, \theta, r, \text{ш})\,\mathrm{d}\text{ш}$$

the latter showing the link between the extended NDF and the usual (filtered) NDF. In the following the extended NDF is simply noted $\overline{f}\,(t, \boldsymbol{x}; \boldsymbol{c}, \theta, r, \text{ш})$. It follows a new kinetic equation:

$$\partial_t \overline{f} + \partial_{\boldsymbol{x}} \cdot (\boldsymbol{c}\overline{f}) + \partial_{\boldsymbol{c}} \cdot (\widehat{\mathbf{F}}\overline{f}) + \partial_\theta \left(\widehat{\frac{H}{c_{p,l}}} \overline{f} \right) + \partial_r (\widehat{R_r}\overline{f}) + \partial_{\text{ш}} (\widehat{R_{\text{ш}}}\overline{f}) = \overline{\mathfrak{B}(f)} + \overline{\mathfrak{C}(f,f)} \tag{5}$$

where the filtered terms are NDF-weighted averages and therefore unclosed: as said previously these terms are expected to be very different from the dilute DNS closures. It is especially irrelevant to compute the LES terms with the DNS terms evaluated with the resolved gas and particle phase fields i.e. $\widehat{\mathbf{F}}(\boldsymbol{c},\boldsymbol{u}_g)$ # $\mathbf{F}(\boldsymbol{c},\widetilde{\boldsymbol{u}_g})$. In the case of a linear drag term, the filtering straightforward brings $\mathbf{F}(\widehat{\boldsymbol{c},\boldsymbol{u}_g}) = \mathbf{F}(\boldsymbol{c},\widehat{\boldsymbol{u}_g})$ which justifies the choice, described above, of adding $\boldsymbol{u}_{g@p}$ to the phase space, therefore just being a model for $\widehat{\boldsymbol{u}_g}$. For non-linear drag however, it is complex to model the evolution of such a seen velocity and it becomes irrelevant to solve for it separately from the actual gas velocity $\widetilde{\boldsymbol{u}_g}$ in a two-way coupling context. Conversely, the seen velocity can be rebuilt from the knowledge of the segregation and ш can also be used to close as well $\widehat{H/c_{p,l}}$, $\widehat{R_r}$, $\overline{\mathfrak{B}}$, and $\overline{\mathfrak{C}}$. Eq. (5) is interpreted as a one-point PDF description of a "cloud of sprays", the statistical particles now being groups of particles characterized at $(t,\boldsymbol{x})$ by their filtered velocities, temperatures, sizes and segregations $(\boldsymbol{c},\theta,r,\text{ш})$.

2.4 Reduction of the EFFK formalism

The NDF has a high dimensional phase space (6D in addition to the 4D of space and time) so it has to be reduced with some assumptions. Resorting to size-conditioning like in Multi-Fluid techniques [12] is an efficient approach because drop size is a dominant parameter of the behavior of the spray. However, two way coupling introduces a strong non-linearity at the local level, making size-conditioned closures less efficient. The treatment of a filtered two-way coupled polydisperse problem is therefore difficult and out of the scope of this contribution. In the following, we fall back to the problem of a monodisperse spray, keeping in mind that Multi-Fluid approaches will probably require a dedicated modeling of the subfilter segregation, its origin and its effects. We also neglect evaporation, break-up, collisions and coalescence so that the system reads:

$$\left\{\begin{array}{ll}
\partial_t\overline{\rho_g}\widetilde{Y_i} + \partial_{\boldsymbol{x}}\overline{\rho_g}\widetilde{Y_i}\widetilde{\boldsymbol{u}_g} & = -\partial_{\boldsymbol{x}}(\mathrm{q}_i + \mathrm{q}_i^{sfs}) + \omega_i \quad , \qquad i \in [\![1; N_{\text{species}}]\!] \\
\partial_t\overline{\rho_g}\widetilde{\boldsymbol{u}_g} + \partial_{\boldsymbol{x}}\rho_g\widetilde{\boldsymbol{u}_g}\otimes\widetilde{\boldsymbol{u}_g} & = -\partial_{\boldsymbol{x}}\widetilde{p} - \partial_{\boldsymbol{x}}(\mathrm{T} + \mathrm{T}^{sfs}) + -\sum_k \widehat{\mathbf{F}}_k \\
\partial_t\overline{\rho_g}\widetilde{e_g} + \partial_{\boldsymbol{x}}\overline{\rho_g}\widetilde{e_g}\widetilde{\boldsymbol{u}_g} & = -\widetilde{p}\partial_{\boldsymbol{x}}\widetilde{\boldsymbol{u}_g} - \partial_{\boldsymbol{x}}(\mathrm{q} + \mathrm{q}^{sfs}) + \sum_k \left(-\widehat{\mathrm{H}}_k + \widehat{\mathbf{F}}_k(\widetilde{\boldsymbol{u}_g} - \widehat{\boldsymbol{u}_k})\right) \\
\partial_t\overline{\boldsymbol{M}_k} + \partial_{\boldsymbol{x}}\overline{\boldsymbol{M}_k}\widehat{\boldsymbol{u}_k} & = 0 \\
\partial_t\overline{m_k}\widehat{\boldsymbol{u}_k} + \partial_{\boldsymbol{x}}\overline{m_k}\widehat{\boldsymbol{u}_k}\otimes\widehat{\boldsymbol{u}_k} & = \widehat{\mathbf{F}}_k \\
\partial_t\overline{m_k}\widehat{h_k} + \partial_{\boldsymbol{x}}\overline{m_k}\widehat{h_k}\widehat{\boldsymbol{u}_k} & = \widehat{\mathrm{H}}_k \\
\partial_t\overline{m_k}\widehat{\text{ш}_k} + \partial_{\boldsymbol{x}}\overline{m_k}\widehat{\text{ш}_k}\widehat{\boldsymbol{u}_k} & = \widehat{R}_{\text{ш}}
\end{array}\right. \tag{6}$$

with $\overline{\boldsymbol{M}_k} = (...,\overline{m_k},...)$ containing as many size moments as needed to reach a good accuracy on the size distribution [6] and k designating the unique liquid section with droplets of the same size r_l. The gas equations feature the turbulent species flux q_i^{sfs}, the turbulent stress tensor $\mathrm{T}^{\mathbf{sfs}}$, and the turbulent heat flux $\mathrm{q}^{\mathbf{sfs}}$ to be modeled specifically in the two-way coupled context while the usual molecular transport terms q_i, T, and q can be treated as usual in LES. Most importantly the filtered spray terms $\widehat{\mathbf{F}}$ and $\widehat{\mathrm{H}}$ should receive a new modeling including the effect of segregation $\widehat{\text{ш}_k}$.

3 A closure for segregation

3.1 Bimodality and upper bound of segregation

For a monodisperse spray the definition of segregation from Eq. (4) simply reads $\widehat{\text{ш}_k} = \frac{\langle\, m_k^2\,\rangle_x}{\overline{m_k}^2}$ with m_k the subfilter mass concentration field that retrieves $\overline{m_k} = \langle\, m_k\,\rangle_x$. Let us introduce the mass concentration sub-PDF $f^s(m_k)$ which is a one-point PDF describing the probability of having a mass concentration $m_{k,loc}$ at a given location. This PDF simply recasts the full DNS information in a non-spatial way, losing track of the space correlations, gradients *etc.* In the following of this section, the filer is a top-hat function over the whole physical space volume $\Omega = \Delta_x^3$ so that $g(\boldsymbol{x}-\boldsymbol{x}') = \frac{1}{\Omega}$. A particular configuration where the spray has a finite mass concentration $m_{k,loc}$ in some areas and is zero elsewhere (on/off) so that

$$m_k(t,\boldsymbol{x}) = \rho_l\mathcal{V}(r_l)f(t,\boldsymbol{x}) = \left\{\begin{array}{ll} 0 & \text{if} \quad \boldsymbol{x}\in\Omega_{\bar{l}} \\ m_{k,loc} & \text{if} \quad \boldsymbol{x}\in\Omega_l \end{array}\right.$$

with $\Omega = \Omega_l + \Omega_{\bar{l}}$ simply translates into a bimodal mass concentration sub-PDF:

$$f^s(m_k) = \frac{\Omega_{\bar{l}}}{\Omega}\delta(m_k) + \frac{\Omega_l}{\Omega}\delta(m_k - m_{k,loc}). \tag{7}$$

The filtered mass concentration does not see the regions of actual higher mass concentrations: $\overline{m_k} = \frac{\Omega_l}{\Omega} m_{k,loc} < m_{k,loc}$. But thanks to the assumption of bimodality, the local value can be retrieved from segregation:

$$m_{k,loc} = \overline{m_k}\widehat{\mathrm{III}_k}. \tag{8}$$

At the microscopic level, $\rho_{l,loc}$ is limited by the behavior of the liquid i.e. $\rho_{l,loc} \leq \rho_l$ with equality when the spray is fully coalesced. Therefore segregation is also limited, depending on the average mass concentration in the filter vicinity with

$$\widehat{\mathrm{III}_k} < \mathrm{III}_{\max} = \frac{\rho_l}{\overline{m_k}} \tag{9}$$

translating the conservation of volume. Since volume occupancy is not accounted for in our moderately dense spray framework, this condition must be enforced in all the subfilter models. As a remark for particle-laden flows, the maximum value of $\rho_{l,loc}$ can be driven by maximum packing or be even more restricted (e.g. by granular pressure) if collisions occur. Finally the bimodality assumption is a key assumption for the modeling of segregation source below and for the modeling of segregation consequences in the next section.

3.2 A priori studies in Taylor-Green vortices

We now perform direct numerical simulations of two-phase turbulence in order to close the evolution of segregation. Studies of turbulence modulation by particles have been previously conducted, especially in homogeneous isotropic contexts [3, 14]. We consider Taylor-Green vortices, a model of free two-phase turbulence, as more representative of subfilter configurations that arise in LES, which are intrinsically transient due to the large scale unsteadiness. Several point-particle computations are led with Raptor, a code developed by Oefelein [15] and the configuration keys are explicated in Table 3.2.

SP	single-phase (gas alone)
1w	two-phase one-way coupled (equivalent to a loading $C = 0$)
2w	two-phase two-way coupled (with a loading $C = 0.5$)
2DTGV0	2D Taylor-Green vortices initial velocity field (frozen, 128^2)
2DCTGV	2D compressible Taylor-Green vortices (128^2)
3DCTGV	3D compressible Taylor-Green vortices (64^3)

Table 1: Key to the numerical configurations.

3.2.1 Taylor-Green Vortices as a model of free turbulence

Taylor and Green [20] consider a simple flow for the maturation of single-scale vortices towards a turbulent flow with $\boldsymbol{u}(t = 0) = (A\sin(ax)\cos(by)\cos(cz), B\cos(ax)\sin(by)\cos(cz), C\cos(ax)\cos(by)\sin(cz))$ and the field is divergence free iff $Aa + Bb + Cc = 0$. We consider the evolution of this initial velocity field under the compressible conditions suggested by [4] i.e. Re = 1600, Ma = 0.08, $a = b = c = L$ and $A = -B = U$ while $C = 0$. The main length scale L is linked to the size L_b of the box $L = L_b/(2\pi)$ and the main time scale is the large eddy turnover time noted τ_{TG}. For the particles, we choose a uniform repartition at zero velocity.

The initial state of this flow, limited to 2D by considering only the x and y axes and referred to as 2DTGV0, has been used as a benchmark for Eulerian models of sprays [5] for its ability to generate complex spray

	Bull and Jameson 2014	"Spray A" SFS
L_b	2π	60×10^{-6} m
U	1	51.5 m/s
τ_{TG}	1	1.16×10^{-6} s
Ma	0.08	0.08
Re	1600	1606
η	3.95×10^{-3}	3.77×10^{-8} m

$d_l = 2r_l$	1.014×10^{-6}	0.717×10^{-6}	0.507×10^{-6}
$\mathrm{St}_L/\mathrm{St}_c$	20	10	5
$\mathrm{Re}_{d,U}$	275.1	194.5	137.5
S-N corr	8.1	6.6	5.4
C	0.5	0.5	0.5
St_L^{2-way}	0.614	0.434	0.307
$N_{spheres}^{box}$	757	2141	6058

Table 2: Parameters of SP-3DCTGV (left) and parameter analysis for the two-phase cases (right).

patterns. In 2DTGV0, the critical Stokes number is analytically derived as being $\mathrm{St}_c = (8\pi)^{-1}$. A simplified cas referred to as 2DCTGV consists in letting evolve this flow in a 2D slice while freezing the evolution of the third component this allows to fully compute the effects of two-way coupling but very little turbulence is of course present. Finally the behavior of the gas phase alone is given in Figure 1 to exhibit the progressive appearance of smaller and smaller scales. A case [4] has been adapted to match the typical subfilter scale imposed in an LES of the so-called Spray A case. Spray A is one of the target cases of the Engine Combustion Network, being both experimentally studied [18] and numerically computed. A recent study [7] exhibits the interest of computing such an injector problem with a mesh resolved by about a tenth of the nozzle diameter so the two-phase subgrid scales must be modeled. Table 2 gives the adaptation of 3DCTGV to feed a subfilter model for such Spray A LES, taking the values from [7] for the choice of the length and velocity scales.

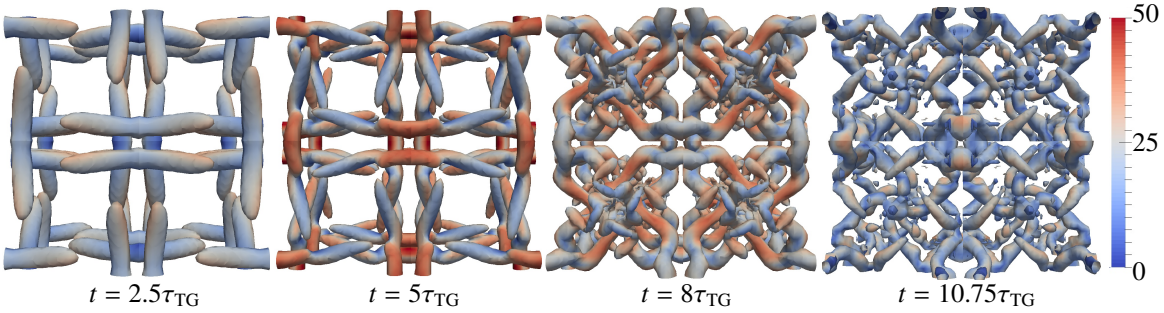

Figure 1: SP-3DCTGV solution showing iso surfaces of Q criterion colored by velocity magnitude (m/s).

3.2.2 Proof of concept of an *a priori* modeling strategy: 2D studies

Only 3D results can be trusted for SFS modeling since the structure of turbulence is dimension-specific. But we first assess the modeling strategy on 2D cases as a proof of concept. We present in Figure 2 the well known patterns of 1w-2DTGV0 to illustrate the complexity of this model problem, even for one-way coupling. But the novelty is the analysis of 2w-2DCTGV, for which time evolution is given in Figure 3 for a chosen Stokes number. In this case, the streaks of particles that are formed shortly after the beginning of the rotation ($t \sim \tau_{\mathrm{TG}}$) are made more stable by two-way coupling, compared to the one-way coupled case where particles immediately spread. This behavior allows a stronger segregation to take place from the beginning and it matches the observations in rapid granular flows [1]. The ability of strips of dense spray to strongly lower the local slip velocity and stabilize together is one of the origins of clustering. In this two-way coupled (2D) turbulent simulation, the symmetry of the configuration is clearly broken; our periodic boundary conditions become inappropriate but we consider that the solution which is provided is still good enough for the purpose of segregation estimation, provided that the streaks of particle in the center (correctly resolved) have the same order of local concentration and thickness as the ones at the boundaries (incorrectly resolved). We plot in Figure 5, left the evolution of segregation versus time for the 2D computations we have run. It is observed that segregation grows continuously and it is higher for St closer to St_c. Also segregation is higher for the two-way coupled cases.

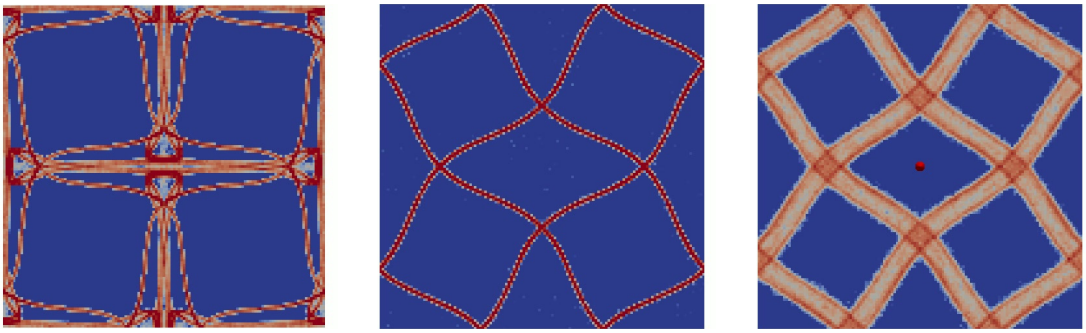

Figure 2: Mass concentration patterns (log-scale) at equilibrium for 1w-2DTGV0 – Left: $\mathrm{St} = 5\mathrm{St}_c$; Middle: $\mathrm{St} = 10\mathrm{St}_c$; Right: $\mathrm{St} = 20\mathrm{St}_c$.

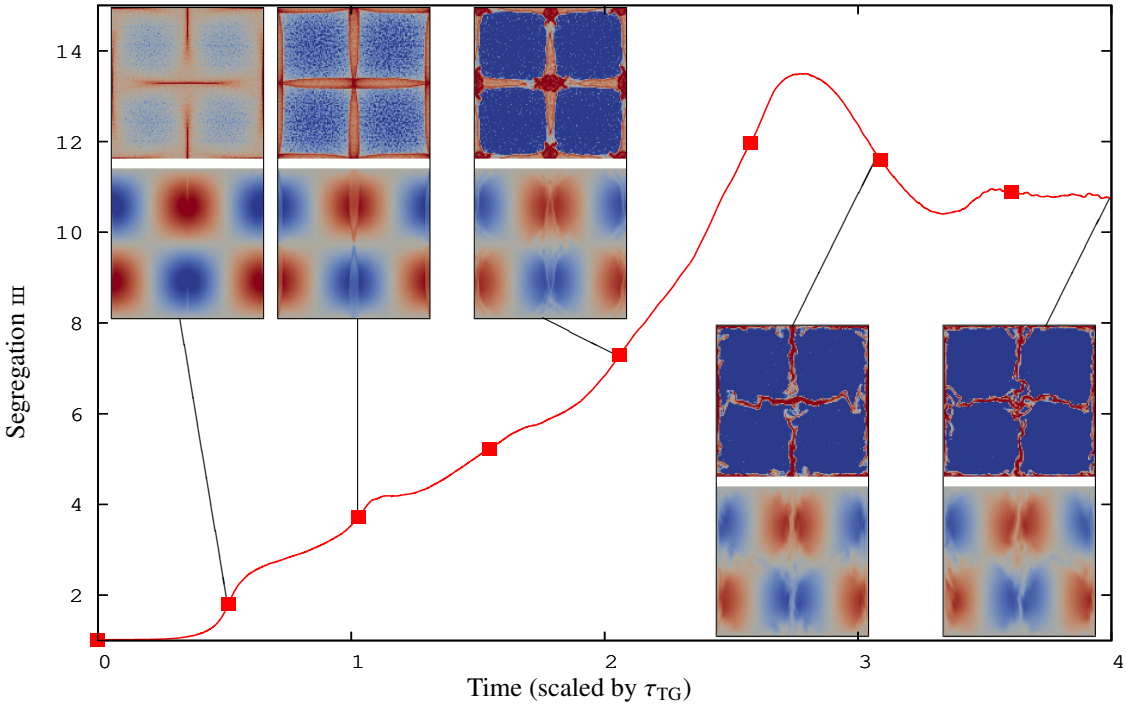

Figure 3: Time evolution of segregation for 2w-2DCTGV with St = 5St$_c$ and corresponding mass concentration pattern (log-scale) and gas velocity component patterns.

3.2.3 *A priori* modeling from 3D simulations

We now present results for the two-phase 3DCTGV case. Some characteristic scales are given in Table 2, (right). The time evolution of 2w-3DCTGV is given in Figure 4, showing clusters to form and then the particle concentration becoming less clustered and uneven at smaller scale. We have run 6 cases in total and the results are given in Figure 5, right. Segregation evolves in a radically different way compared to 2DCTGV: (i) the values are lower, (ii) a maximum appears after a couple of τ_{TG}, (iii) it appears later for higher St, and (iv), though 2w has higher segregation as 1w at the beginning, segregation decreases with an exponential behavior in a way that seems St-dependent but not related to C. These observations give hope that a robust closure can be introduced for $\widehat{R_{III}}$ but the dependence on loading C must be further investigated.

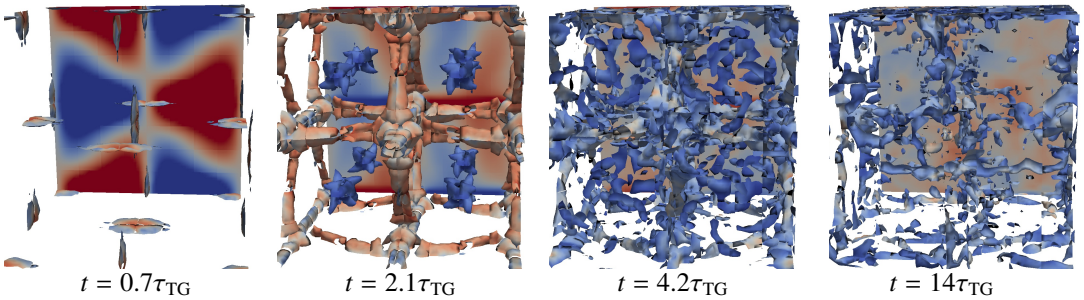

Figure 4: Time evolution of 2w-3DCTGV with St = 5St$_c$ showing iso-surfaces of $\overline{m_k}$ = 30 kg/m^3 colored by liquid velocity variance – Background slice plane shows the axial velocity of the gas.

4 Segregation-based dense spray closures

We show the key role of mass loading on the dynamics of momentum and heat transfers. We then assess the relevance and merits of the so-called scale separation assumption in simplifying the description of subfilter spray dynamics. This assumption backs the derivation of segregation-dependent filtered source terms $\widehat{\mathbf{F}}$ and $\widehat{\mathrm{H}}$.

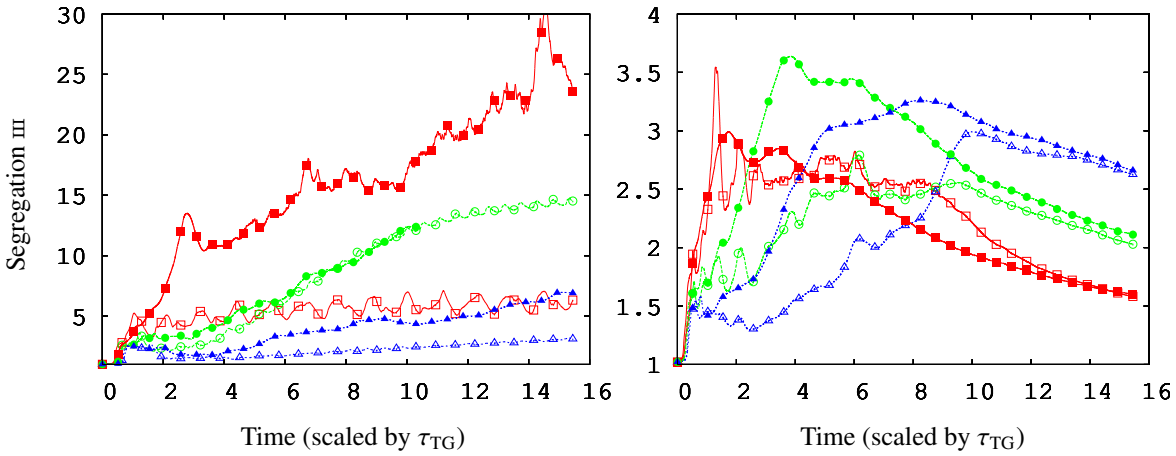

Figure 5: Time evolution of segregation (Left: 2DCTGV ; Right: 3DCTGV) for 1w (hollow symbols) and for 2w (solid symbols) – □: St = 5St$_c$; ○: St = 10St$_c$; △: St = 20St$_c$.

4.1 Motivating the choice of segregation

4.1.1 Non-smoothness of subfilter fields

In the context of LES, subfilter non-uniformities of the liquid (clusters) can appear so that the momentum and heat transfers must be corrected in terms of dynamics and equilibrium. By studying circulating fluidized bed statistics [17] closes a "seen" velocity with the local quantities $\widehat{u_g}^{\text{corr}} = \frac{\Delta x^2}{12}\partial_{x_j}\alpha_p\partial_{x_j}\widehat{u_g} + O(\Delta x^4)$. They assume that the subfilter variations can be described by the resolved derivatives. From a mathematical point of view this is relevant in the case of a quasi-DNS so that the fully resolved field is slightly more corrugated than the resolved one and can be approximated by low order Taylor expansion terms. But in LES, the subfilter field can be very rough, requiring an unrealistically high order term to describe it, and potentially missing some couplings. From a physical point of view, there is little evidence of any scale similarity in segregation that could bring the first resolved derivatives to quantitatively render some small scale variations. In the following, we identify the importance of mass loading and suggest a closure that cuts loose from regularity assumptions and space correlations, only seeking the independent effects of the various loadings present at the subfilter levels on scale-separated regions of the subfilter flow.

4.1.2 Role of loading on heat and momentum transfer dynamics

Let us consider a 0D two-phase problem: a mixture of gas and liquid (mass concentrations m_g and m_l respectively) with a difference of velocities (u_g and u_l). The two-way coupled momentum system reads, both in primitive and in characteristic form:

$$\begin{cases} \partial_t(m_g u_g) = \dfrac{m_l}{\tau}\left(u_l - u_g\right) \\ \partial_t(m_l u_l) = -\dfrac{m_l}{\tau}\left(u_l - u_g\right) \end{cases} \qquad (10) \qquad \begin{cases} \partial_t\left(m_g u_g + m_l u_l\right) &= 0 \\ \partial_t\left(u_l - u_g\right) &= -\dfrac{1+C}{\tau}\left(u_l - u_g\right) \end{cases} \qquad (11)$$

with a linear drag for the sake of simplicity. The equilibrium state is $u_l = u_g = u_{\text{eq}}$ at $t \to +\infty$ with $u_{\text{eq}} = \frac{m_g u_g + m_l u_l}{m_g + m_l}$. The control parameter of the study is the mass loading $C = \frac{m_l}{m_g}$. While for $C \ll 1$ the characteristic time was obviously $\tau^{\text{1-way}} = \tau$, the two-way coupled System (10) has a characteristic time (non-trivial eigenvalue of the characteristic system Eq. (11)) which decreases with the loading, as stated by [6]:

$$\tau^{\text{2-way}}(C) = \frac{\tau}{1+C}. \qquad (12)$$

The dependency of the dynamics on the loading is not visible from the analysis of the drag force itself: especially here where it is taken as a simple linear force, solely depending on the velocity difference. On the contrary, the sensitivity to loading is a property that emerges from the non-linearity of the two-way coupled system. It plays a crucial role in the dynamics of two-phase flows, being even stronger when clustering occurs. So this effect must be accounted for at the level of resolved velocities to close the filtered drag $\widehat{\mathbf{F}}$. The same non-linearity of the characteristic time appears in heat transfer processes since the 0D system has the same structure so that the filtered heat transfer $\widehat{\mathrm{H}}$ encounters the same closure peculiarity.

4.1.3 Scale separation, local equilibria and space filtering

Recognizing that the subfilter fields have deeply unresolved scales and that the local loading has a dominant effect on transfer dynamics, we rely on a simplified subfilter configuration for closure purpose, where the two-way coupling time can be assessed from an estimate of the local mass concentrations at various points of the subfilter level while the influence of the exact subfilter structures (gradients, two-point information) is neglected. This approach corresponds to a one-point PDF description of the subfilter spray.

We consider a collection $k \in [1, N]$ of 0D two-phase problems with the quantities $m_{g,k}$, $u_{g,k}$, $m_{l,k}$, and $u_{l,k}$: this can correspond to a non-uniform two-phase flow, described as sub-domains at space locations that are far enough not to exchange momentum over the considered time (scale separation). With this "disconnection" assumption, the exact problem is then solved by finding the local equilibria for each system separately:

$$\begin{cases} \partial_t m_{g,k} u_{g,k} = \dfrac{m_{l,k}}{\tau}\left(u_{l,k} - u_{g,k}\right) \\ \partial_t m_{l,k} u_{l,k} = -\dfrac{m_{l,k}}{\tau}\left(u_{l,k} - u_{g,k}\right). \end{cases} \tag{13}$$

Averaging over k is then equivalent to filtering over the whole domain so that we can consider the following as being our filtered problem and filtered quantities:

$$\begin{cases} \partial_t \overline{m_g}\widehat{u_g} = \dfrac{1}{\tau}\left(\overline{m_l}\widehat{u_l} - \overline{m_l u_g}\right) \\ \partial_t \overline{m_l}\widehat{u_l} = -\dfrac{1}{\tau}\left(\overline{m_l}\widehat{u_l} - \overline{m_l u_g}\right) \end{cases} \tag{14}$$

$$\overline{m_g} = \frac{1}{N}\sum m_{g,k}\ , \quad \overline{m_g}\widehat{u_g} = \frac{1}{N}\sum m_{g,k}u_{g,k}\ ,$$
$$\overline{m_l} = \frac{1}{N}\sum m_{l,k}\ , \quad \overline{m_l}\widehat{u_l} = \frac{1}{N}\sum m_{l,k}u_{l,k}\ .$$

where the term $\overline{m_l u_g}$ cannot be expressed from the standard filtered quantities. In the case of a non-linear drag, the troublesome filtered term is $\overline{m_l \boldsymbol{F}(u_l, u_g)}$. Naïvely taking $\overline{m_l u_g} = \overline{m_l}\widehat{u_g}$ is equivalent to solving a momentum relaxation with the filtered quantities (the "no-model" model). It is expected that the dynamics will not be respected according to the conclusions of Section 4.1.2. But worse is the fact that the naïve system will predict an equilibrium: this is erroneous since a non-uniform problem is not expected to reach such a global equilibrium over short times.

Let us consider an example where the liquid is segregated in 10% of the domain while $\overline{m_g} = \overline{m_l}$ i.e. $\overline{C} = 1$ on average in the domain. We therefore have a maximum of $C = 10$ where the liquid is present. The computed results are given in Figure 6 (left) where it is obvious that the dynamics and equilibrium are different for the exact problem after averaging compared to the naïve resolution of the problem.

4.2 A first subfilter model for momentum and heat transfers

4.2.1 Scale-separation bimodal subfilter closures

If scale separation occurs and allows local equilibria over the time scale of observation, the filtered drag force should be computed with respect to a certain knowledge of the segregation level. Provided the segregation factor in the domain: $\text{Ш} = \frac{\frac{1}{N}\sum m_{l,k}^2}{\left(\frac{1}{N}\sum m_{l,k}\right)^2} = N\frac{\sum m_{l,k}^2}{\left(\sum m_{l,k}\right)^2}$ we can assess a ratio of segregated volume, i.e. the volume where the spray actually sits at the subfilter level: $\nu = 1/\text{Ш}$ and compute the evolution of the liquid velocity assuming that it is concentrated in a sub-domain with a fraction ν of the domain's volume: as a consequence, the liquid will exchange momentum with only a fraction ν of the gas, the remaining part $(1-\nu)\overline{m_g}$ remaining at its initial velocity $\widehat{u_g^0}$. With this assumption, the averages converge towards two different values in the phase:

$$\begin{aligned} \widehat{u_l}^{\text{eq}} &= \frac{\nu\overline{m_g}\widehat{u_g} + \overline{m_l}\widehat{u_l}}{\nu\overline{m_g} + \overline{m_l}}, \\ \widehat{u_g}^{\text{eq}} &= \nu\widehat{u_l}^{\text{eq}} + (1-\nu)\widehat{u_g} \end{aligned} \tag{15}$$

which renders the fact that part of the gas does not see the liquid. As for the computational aspects, the approach simply requires to compute the drag force as follows for both equations:

$$\overline{m_l \boldsymbol{F}(u_l, u_g)} = \overline{m_l}\widehat{\mathbf{F}}(\widehat{u_l}, \widehat{u_g}^{\text{corr}}) \quad \text{with} \quad \widehat{u_g}^{\text{corr}} = \widehat{u_g^0} + \frac{1}{\nu}(\widehat{u_g} - \widehat{u_g^0}) \tag{16}$$

whatever the form of the drag, so that the gas initial velocity $\widehat{u_g^0}$ in the cell must be stored. Such an approach is conservative (same drag term for both phases) and it respects the difference in average velocities at equilibrium.

With this model, the result shown in Figure 6 (right) proves to be satisfactory: the model matches exactly the reference if the liquid is effectively homogeneous in the sub-domain (bimodality). In the limit of a null

segregation, corresponding to a perfect repartition of the liquid in the domain $\nu = 1$, it is obvious from the equation that the model exactly recovers the average system, also equal to the DNS system. In the limit of a particle loading C low enough for non-linear two-way coupling to vanish, the modified equation behaves as the DNS one as regards the little evolution of $\widehat{u_l}(t) \approx \widehat{u_g^0}$ along time because C is still in factor of the (modified) source term in the velocity equation so that the seen gas velocity $\widehat{u_g}^{\text{corr}} \approx \widehat{u_g^0}$ remains constantly equal to the initial average gas velocity: the particle velocity then evolves as the DNS particle velocity would and as a result the whole system behaves as the DNS one, whatever the value of the segregation, which is the expected behavior in one-way coupling.

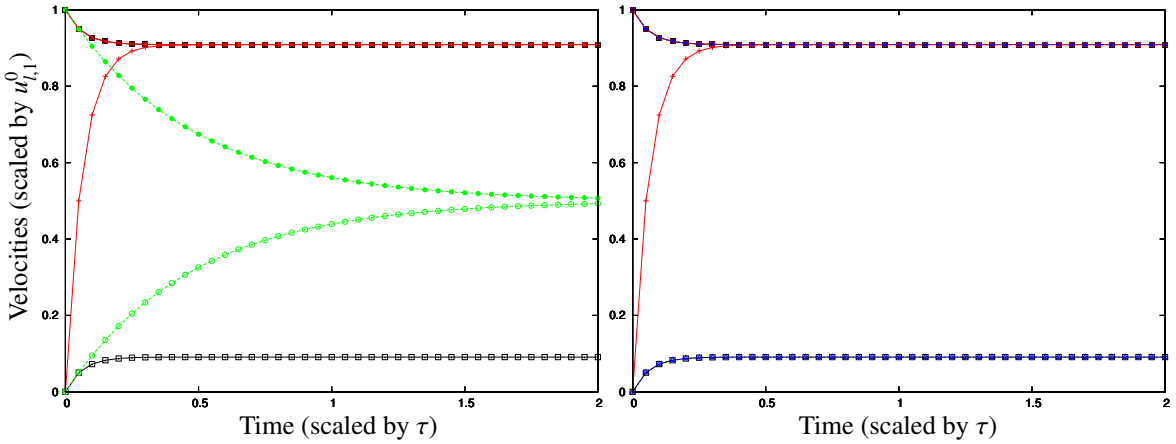

Figure 6: Evolution of velocities for a bimodal collection of 0D two-phase problems – Velocities in the sub-domain where $C = 10$ (+ for $u_{g,1}$ and × for $u_{l,1}$); Exact velocities average over the domain (□ for $\widehat{u_g}$ and ■ for $\widehat{u_l}$); Left: Naïve resolution of the average problem (○ for gas and ● for liquid); Right: Corrected resolution of the average problem (△ for gas and ▲ for liquid).

4.2.2 Effect of non-bimodal mass concentration sub-PDFs

To assess the validity of the assumption of bimodality of the mass concentration sub-PDF, we solve for a scale-separated problem with more than one values of loading. Results are presented in Figure 7 (right) for a particular case of an inhomogeneous segregation with a ratio of 9 to 1 in two sub-domains and they are satisfactory. The sub-PDFs yielding the worst discrepancies for our model have not been determined but the fact that things go well in a non-bimodal case provides a first test case. The robustness of the bimodal assumption presumably comes from the strong non-linearity of the two-way coupled characteristic time so that the highest concentration region has a dominant effect on the dynamics.

4.2.3 Beyond the scale-separation assumption

If the scale separation assumption is valid (i.e. liquid clusters only interact with their local counterpart of gas), then the model is exact if the gas velocity is split into a component that has never seen the particles, constant to $\widehat{u_g^0}$, and a component that has seen the particles and is easily reconstructed from momentum conservation:

$$\widehat{u_{g@p}} = \frac{1}{\nu}\left(\widehat{u_g} - (1-\nu)\widehat{u_g^0}\right) = \widehat{u_g}^{\text{corr}}.$$

Considering $\widehat{u_g}$ and $\widehat{u_l}$ as the standard LES velocities this information of two gas velocities is lost as soon as the knowledge of $\widehat{u_g^0}$ is lost, e.g. at the beginning of a new time step in a dual time-stepping context. If the information is reset as shown in Figure 7 (right), it results in a partial mixing (diffusion) of the gas and liquid momenta, which is physical: this process relaxes the scale-separation assumption. In this early model, the rate of mixing or "scale interaction" occurs at a rate that is driven by the time step, therefore possibly not physically sound. A more advanced model would require the storage of the "seen" velocity and its relaxation according to a second characteristic time to be determined. The latter is presumably driven by the intermediate structures of two-phase turbulence (the largest at the subfilter level).

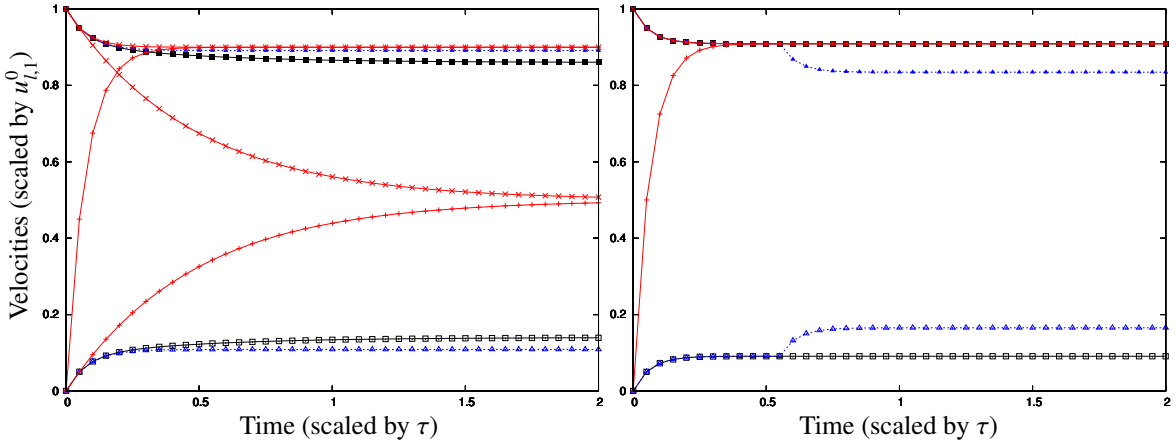

Figure 7: Evolution of velocities for a non-bimodal (left) and a bimodal (right) collection of 0D two-phase problems – Velocities in the sub-domains where $C = 9$ and 1 (left) and $C = 10$ (right) ($+$ for $u_{g,i}$ and $\times$ for $u_{l,i}$); Exact velocities average over the domain ($\square$ for $\widehat{u_g}$ and $\blacksquare$ for $\widehat{u_l}$); Left: Corrected resolution of the problem averaged from $C = 9$ and 1 ($\triangle$ for gas and $\blacktriangle$ for liquid); Right: Corrected resolution of the problem averaged from $C = 10$ with $\widehat{u^0_g}$ reset after 0.55τ ($\triangle$ for gas and $\blacktriangle$ for liquid).

4.3 Conclusion on the filtered term closures

Describing segregation is a possible path to work out the NDF-filtered quantities and the evolution of segregation itself can be modeled with a physically sound closure from the systematic processing of *a priori* DNS databases, as shown in Section 3. With the sole knowledge of this data, it has been possible to write a closure for drag and heating that reproduces the main feature of two-way coupling, namely its dependence on the local loading. The simplicity of these closures advocates for the transport of segregation in the EFFK formalism devised in Section 2.3. Also the filtered collision terms are expected to be better resolved from the knowledge of segregation since they strongly (quadratically) depend on the local mass concentration. While the filtered break-up terms could benefit from the knowledge of a "seen" velocity to assess the local aerodynamic break-up. We however highlight a caveat in the case of evaporating sprays: the problem of deriving a model for the filtered mass transfer term remains since evaporation depends on the local vapor gradients, which might not be easily computed in the absence of any knowledge of the subfilter space structures. The scale separation assumption must be completed by the effect of the intermediate range structures on the vapor/combustion fields.

5 Conclusion

A formalism referred to as Extended Filtered Fluid Kinetic (EFFK) has been defined for the LES of dense two-phase flows. We have assessed the case where segregation -a one-point measure of the level of clustering- is taken as sole variable to extend the kinetic formalism. This choice has proven to be reasonable since it can both (i) be closed in terms of the evolution of segregation itself and (ii) ease the modeling of the other filtered terms. Indeed salient facts on the evolution of segregation in free turbulence have been provided as a basis for its closure from *a priori* studies of a model two-phase turbulence configuration. And a segregation-based closure of filtered drag and heating has been performed with a good level of theoretical backing, considering that the dynamics of average velocity and enthalpy is driven by the local values of mass concentration due to two-way coupling non-linearity. As a perspective, the overall model should be *a posteriori* tested and refined to allow the LES of internal combustion engine injection, in particular the Spray A case, in the context of the Engine Combustion Network workshops.

References

[1] K. Agrawal, P. N. Loezos, M. Syamlal, and S. Sundaresan. The role of meso-scale structures in rapid gas–solid flows. *Journal of Fluid Mechanics*, 445:151–185, 2001.

[2] S. Balachandar and J.K. Eaton. Turbulent dispersed multiphase flow. *Annual Review of Fluid Mechanics*, 42:111–133, 2010.

[3] M. Boivin, O. Simonin, and K. D. Squires. Direct numerical simulation of turbulence modulation by particles in isotropic turbulence. *Journal of Fluid Mechanics*, 375:235–263, 1998.

[4] J.R. Bull and A. Jameson. Simulation of the Compressible Taylor Green Vortex using High-Order Flux Reconstruction schemes. In 7th *AIAA Theoretical Fluid Mechanics Conference*, Atlanta, GA, 2014.

[5] S. de Chaisemartin. *Polydisperse evaporating spray turbulent dispersion: Eulerian model and numerical simulation*. PhD thesis, Ecole Centrale Paris, 2009. http://tel.archives-ouvertes.fr/tel-00443982/en/.

[6] F. Doisneau. *Eulerian modeling and simulation of polydisperse moderately dense coalescing spray flows with nanometric-to-inertial droplets: application to Solid Rocket Motors*. PhD thesis, École Centrale Paris, 2013.

[7] F. Doisneau, M. Arienti, and J. C. Oefelein. Study of the momentum coupling between liquid fuel and ambient gas during injection using a dense spray formulation. In 9th *US National Combustion Meeting*, pages 1–11, Cincinnati, USA, 2015.

[8] K. Domelevo and P. Villedieu. A hierarchy of models for turbulent dispersed two-phase flows derived from a kinetic equation for the joint particle-gas PDF. *Commun. Math. Sci.*, 5(2):331–353, 2007.

[9] S. Elghobashi. Particle-laden turbulent flows – Direct simulation and closure models. *App. Sc. Research*, 38:301–314, 1991.

[10] P. Fevrier, O. Simonin, and K.D. Squires. Partitioning of particle velocities in a gas-solid turbulent flow into a continuous field and a spatially-uncorrelated random distribution: theoretical formalism and numerical study. *J. Fluid Mech.*, 533:1–46, 2005.

[11] R. O. Fox. On multiphase turbulence models for collisional fluid–particle flows. *Journal of Fluid Mechanics*, 742:368–424, 2014.

[12] F. Laurent and M. Massot. Multi-fluid modeling of laminar poly-dispersed spray flames: origin, assumptions and comparison of the sectional and sampling methods. *Comb. Theory and Modelling*, 5:537–572, 2001.

[13] E. Masi. *Étude théorique et numérique de la modélisation instationnaire des écoulements turbulents anisothermes gaz-particules par une approche Euler-Euler*. PhD thesis, Institut National Polytechnique de Toulouse, 2010.

[14] R.S. Miller and J. Bellan. Direct numerical simulation and subgrid analysis of a transitional droplet laden mixing layer. *Phys. Fluid*, 12(3):650–671, 2000.

[15] J. C. Oefelein. Large Eddy Simulation of turbulent combustion processes in propulsion and power systems. *Progress in Aerospace Sciences*, 42(1):2–37, 2006.

[16] A. Ozel, P. Fede, and O. Simonin. Development of filtered Euler–Euler two-phase model for circulating fluidised bed: high resolution simulation, formulation and a priori analyses. *International Journal of Multiphase Flow*, 55:43–63, 2013.

[17] J.-F. Parmentier, O. Simonin, and O. Delsart. A functional subgrid drift velocity model for filtered drag prediction in dense fluidized bed. *AIChE Journal*, 58(4):1084–1098, 2012.

[18] L.M. Pickett, C.L. Genzale, J. Manin, L.M. Malbec, and L. Hermant. Measurement uncertainty of liquid penetration in evaporating diesel sprays. *ILASS2011-111*, 2011.

[19] P. Sagaut. *Large Eddy Simulation for Incompressible Flows*. Springer, Berlin, 1998.

[20] G. I. Taylor and A. E. Green. Mechanism of the Production of Small eddies from Large Ones. *Proceedings of the Royal Society of London. Series A, Mathematical and Physical Sciences*, 158(895):499–521, 1937.

[21] Z. Zeren. *Modélisation Lagrangienne stochastique des écoulements gaz-solides turbulents avec couplage inverse en Turbulence Homogène Isotrope stationnaire*. PhD thesis, Institut National Polytechnique de Toulouse, 2010.